

Quantitative Determination of Proteins Based on Strong Fluorescence Enhancement in Curcumin-Chitosan-Proteins System

Feng Wang · Wei Huang · Lingyan Jiang · Bo Tang

Received: 11 July 2011 / Accepted: 14 October 2011 / Published online: 22 January 2012
© Springer Science+Business Media, LLC 2012

Abstract We found that the fluorescence intensity of curcumin (CU) can be highly enhanced by protein bovine serum albumin (BSA) and human serum albumin (HSA) in the presence of chitosan (CTS). Based on this finding, a new fluorimetric method to determine the concentration of protein was developed. Under optimized conditions, the enhanced intensities of fluorescence are quantitatively in proportion to the concentrations of protein in range of 0.007–100 $\mu\text{g}\cdot\text{mL}^{-1}$ for BSA and 0.004–100 $\mu\text{g}\cdot\text{mL}^{-1}$ for HSA at 426 nm excitation, and 0.007–100 $\mu\text{g}\cdot\text{mL}^{-1}$ for BSA and 0.01–100 $\mu\text{g}\cdot\text{mL}^{-1}$ for HSA at 280 nm excitation, while corresponding qualitative detection limits ($S/N=3$) can lower to 3.96, 2.46, 4.56, 9.20 $\text{ng}\cdot\text{mL}^{-1}$, respectively. The method has been successfully used for the determination of HSA in real samples. Based on resonance light scattering and UV-visible absorption spectroscopic analysis, mechanism studies suggested that the highly enhanced fluorescence of CU was resulted from synergic effects of favorable hydrophobic microenvironment provided by BSA and CTS and efficient intermolecular energy transfer between BSA and CU. Protein BSA may bind to CTS through hydrogen bonds, which causes the protein conformation to convert from β -fold to α -helix. CU can combine with

the BSA-CTS complex through its center carbonyl carbon, and CTS plays a key role in promoting the energy transfer process by shortening the distance between BSA and CU.

Keywords Curcumin (CU) · Chitosan (CTS) · Protein · Fluorescence

Introduction

Serum albumins such as bovine serum albumin (BSA) and human serum albumin (HSA) are the most abundant blood plasma protein and forms a large proportion of all plasma protein, which play a significant role in physiological functions by acting as carrier proteins [1–3]. They aid in the transport, distribution and metabolism of many exogenous ligands, which include fatty acids, amino acids, metals, drugs and pharmaceuticals [4–9]. It is well known that BSA has conformational adaptability when binding to various ligands [1–3] including metabolites, drugs, dyes, fatty acids, etc. Chitosan, β -(1–4)-2-amino-2-deoxy- D-glucose (Fig. 1), a natural linear biopolyamino- saccharide is obtained by alkaline deacetylation of chitin, which is the second abundant polysaccharide next to cellulose [10, 11], while chitin is the principal component of protective cuticles of crustaceans such as crabs, shrimps, prawns, lobsters and cell walls of some fungi such as aspergillus and mucor. Chitin is a straight homopolymer composed of β -(1, 4)-linked *N*-acetyl-glucosamine units, while chitosan comprises of copolymers of glucosamine and *N*-acetyl-glucosamine [12–14]. Biodegradable property, low toxicity and good biocompatibility make chitosan very useful in biomedical and pharmaceutical formulations [15, 16].

Curcumin (CU), 1,7-bis (4-hydroxy-3-methoxyphenyl)-1, 6-heptadiene-3, 5-dione (Fig. 2), is the main constituent of

F. Wang (✉) · W. Huang · L. Jiang
Department of Chemistry and Chemical Engineering,
Zaozhuang University,
Zaozhuang 277160, Peoples Republic of China
e-mail: wf332@uzz.edu.cn

F. Wang
e-mail: wf3786621@163.com

B. Tang
College of Chemistry, Chemical Engineering and Materials Science,
Shandong Normal University,
Jinan 250014, Peoples Republic of China

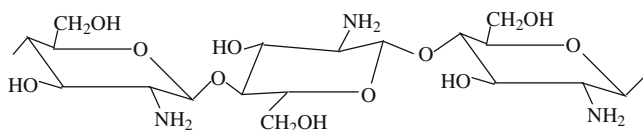


Fig. 1 Chemical structure of chitosan

rhizomes of the plant *curcumin longa*, which is a common ingredient used in spices, cosmetics and traditional Chinese medicine. Recently, CU has attracted much interest because several experimental studies have demonstrated that this natural polyphenol has anti-inflammatory, antineoplastic and anti-angiogenic activities [17, 18].

In previous research, we have found that the fluorescence intensity of CU could be greatly enhanced by proteins (such as BSA and HSA) in the presence of surfactant and rare earth ions. In this research, we further find that the CU fluorescence could be enhanced by protein in the presence of CTS and suggest using CU-CTS complex as a new type of convenient fluorescent probe for proteins. Experimental results indicate that the enhanced fluorescence intensity is proportional to the concentration of proteins over a wide range and their detection limits are at nanogram level. The method has been tested with real samples of people serum.

Experimental

Chemicals

BSA and HSA were purchased from Shanghai Boao Biochemical Technology Co. and Sigma, respectively. Chitosan (MW=150,000) came from Shanghai Junchuang Chemical Co. All the chemicals are analytical grade reagents and deionized water was used for all experiments.

Stock Solutions

Stock solutions of BSA and HSA at $1,000 \mu\text{g}\cdot\text{mL}^{-1}$ were prepared by dissolving them in water. A stock solution of CU at $1.00 \times 10^{-3} \text{ mol}\cdot\text{L}^{-1}$ was prepared by dissolving 0.0368 g of curcumin in ethanol and then diluting it to 100 mL with ethanol. A chitosan solution of $100 \mu\text{g}\cdot\text{mL}^{-1}$ was prepared by dissolving 0.2500 g of CTS into 10% acetic acid and then diluting it with deionized water to 250 mL.

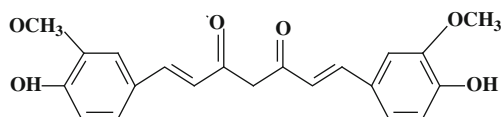


Fig. 2 Chemical structure of curcumin

Britton-Robinson-NaOH (BR-NaOH, $0.10 \text{ mol}\cdot\text{L}^{-1}$) was used for the pH adjustment. These stock solutions were stored at $0-4 \text{ }^\circ\text{C}$ for experiments.

Measurement

Fluorescence spectra were recorded with an F-2500 spectrofluorometer (Hitachi, Japan) and absorption spectra were taken with an UV-2401 spectrophotometer (Shimadzu, Japan). For spectral measurements, all samples were prepared according to the following procedure: 1.00 mL of BR-NaOH (pH 2.50), 0.50 mL of CU ($1.00 \times 10^{-4} \text{ mol}\cdot\text{L}^{-1}$), 2.00 mL of CTS ($1,000 \mu\text{g}\cdot\text{mL}^{-1}$) and certain standard BSA (or sample solution) in turn, and then the mixture was diluted to 10 mL with water and allowed to stand for 15 min. The fluorescence intensity was measured in a 1 cm quartz cell at $\lambda_{\text{ex}}/\lambda_{\text{em}}=426 \text{ nm}/500 \text{ nm}$ and $\lambda_{\text{ex}}/\lambda_{\text{em}}=280 \text{ nm}/500 \text{ nm}$ and with a slit of 10.0 nm for excitation and emission. The enhanced fluorescence intensity of CU-CTS-BSA system were represented as $\Delta I_f = I_f - I_f^0$. Here, I_f and I_f^0 were the intensities of the systems with and without proteins, respectively. The resonance light scattering (RLS) spectra were obtained by simultaneously scanning the excitation and emission monochromators (namely, $\Delta\lambda = 0 \text{ nm}$) of the spectrofluorometer from 220 to 600 nm in a 1 cm quartz cell with a slit of 2.5 nm.

Results and Discussion

Fluorescence Behavior and Optimization of Conditions

The fluorescence spectra of the systems are shown in Figs. 3 and 4. It can be seen that in a BR-NaOH buffer of pH 2.50, CU only exhibits very weak fluorescence with an

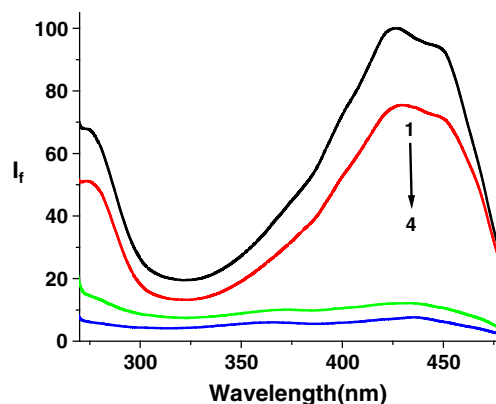
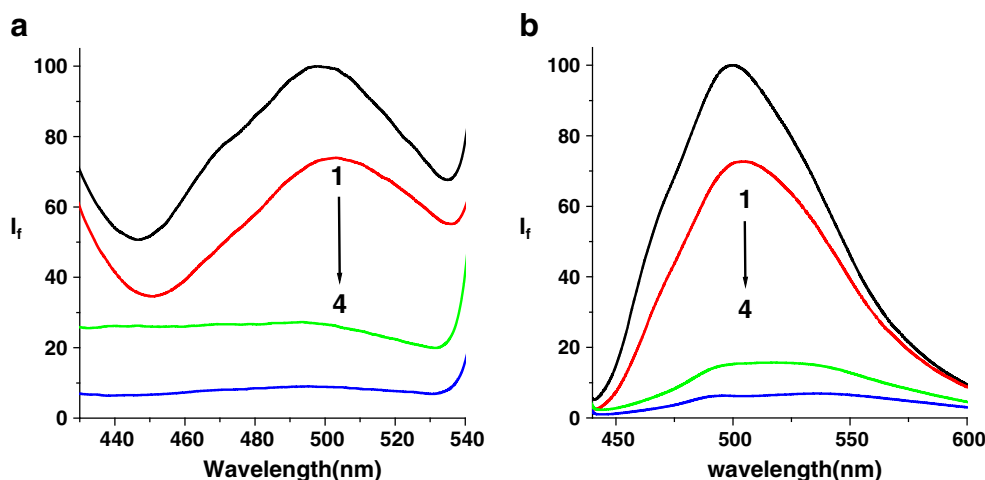


Fig. 3 Fluorescence excitation spectra ($\lambda_{\text{em}}=500 \text{ nm}$) of: (1) CU-CTS-BSA, (2) CU-BSA, (3) CU-CTS, and (4) CU. systems. Conditions: CU: $5.00 \times 10^{-6} \text{ mol}\cdot\text{L}^{-1}$; CTS: $200 \mu\text{g}\cdot\text{mL}^{-1}$; BSA: $100 \mu\text{g}\cdot\text{mL}^{-1}$; pH 2.50

Fig. 4 Fluorescence emission spectra (a. $\lambda_{ex}=280$ nm; b. $\lambda_{ex}=426$ nm) of: (1) CU-CTS-BSA, (2) CU-BSA, (3) CU-CTS, and (4) CU systems. Conditions: CU: 5.00×10^{-6} mol·L⁻¹; CTS: 200 μ g·mL⁻¹; BSA: 100 μ g·mL⁻¹; pH 2.50



excitation peak of 440 nm and an emission peak of 530 nm. After the addition of CTS or BSA, the fluorescence of CU has little enhancement. However, when both CTS and BSA are added to the system, the fluorescence intensity of the CU-CTS-BSA system is significantly higher than that of CU-CTS and CU-BSA systems. Also, with an emission at 500 nm, the excitation peak blue-shifts to 426 nm and a new peak 280 nm appears in CU-BSA and CU-CTS-BSA systems. These phenomena clearly reveal interactions among CU, CTS and BSA. In the CU-CTS-BSA system, experimental conditions were optimized for fluorescence enhancement by finely tuning the pH value, type of buffers, concentrations of CTS and reaction time.

Effects of pH and Buffers

The effect of pH on the fluorescence intensity of the system was tested. The experimental results indicate that the fluorescence intensity enhancement reaches a maximum at pH 2.50. Experiments indicate that different buffers also have a large effect on the fluorescence intensity of the system. The ΔI_f (%) for critic-sodium—HCl, Na₂HPO₄—critic acid, HOAc—NaOAc, glycine—HCl, Tris—HCl, BR—NaOH, Borax—HCl, critic—sodium citrate at pH of 2.50 is 78.05, 85.91, 80.69, 62.29, -12.58, 100.0, -17.22 and 64.16, respectively. The results demonstrate that BR-NaOH is the best of the buffers tested. Thus, the BR—NaOH buffer (pH=

2.50) was selected for the assay, and the optimum volume of BR—NaOH buffer is 1.00 mL.

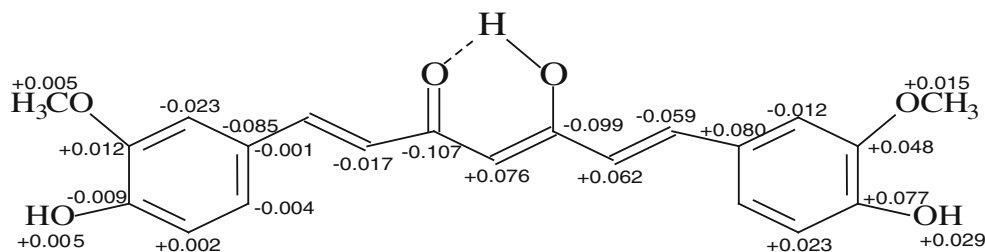
As known, the isoelectric point of BSA is at pH 4.7. BSA is positively charged at pH<4.7 and in this paper pH=2.50, so BSA is positively charged. Chitosan is an amino polysaccharide molecule containing a large number of amino and carboxyl groups, in the acidic environment, the amino proton adsorption became positively charged ions. Figure 5 exhibits differential atomic charges of a curcumin molecule in the first excited state [19]. Positive signs indicate a decrease and negative signs an increase in π -electron density upon electronic excitation to the first excited state. It can be seen that there are maximal electron density at the two carbon atoms of the carbonyl.

Therefore, the positive charge of protein and chitosan may be interacting with carbonyl on the large conjugation system of curcumin by electrostatic force, and then the larger CU-CTS-BSA ternary complex is formed.

Effect of CU

The effect of the concentration of CU on the fluorescence intensity was tested. The fluorescence intensity enhancement reaches its maximum at a CU concentration of 5.00×10^{-6} mol·L⁻¹ and this concentration was chosen for further studies.

Fig. 5 Differential atomic charges of curcumin molecule in the first excited state



Effect of CTS

The fluorescence intensity of the system with various concentrations of CTS was tested and it was found that the fluorescence intensity enhancement effect reaches the maximum when CTS concentration is $2.00 \times 10^{-4} \text{ g}\cdot\text{mL}^{-1}$. Therefore, $2.00 \times 10^{-4} \text{ g}\cdot\text{mL}^{-1}$ of CTS concentration was selected for the assay.

Effect of Reaction Time

Tests show that ΔI_f reached a maximum within 15 min after reagents had been added and remained stable for at least 2 h afterwards. Therefore, the system exhibited good stability. In this research, 15 min of sample incubation time was set for all the fluorescence measurements.

Analytical Performance

With the standard analytical procedure established at the optimized conditions mentioned above, interferences of foreign substances including various ions and biomolecules on fluorescence of the CU-CTS-BSA system were evaluated. The results in Table 1 indicate these foreign

Table 1 Interference from foreign substances

Foreign substances	Concentration ($10^{-7} \text{ mol}\cdot\text{L}^{-1}$)	ΔI_f (%)
Na^+ , Cl^-	2	4.27
Ca^{2+} , Cl^-	1	5.87
NH_4^+ , Cl^-	2	5.03
Zn^{2+} , Cl^-	5	4.36
Mn^{2+} , Cl^-	1	5.11
Na^+ , SO_4^{2-}	2	6.61
K^+ , Cl^-	3	-5.64
Mg^{2+} , SO_4^{2-}	1	5.54
Cu^{2+} , Cl^-	4	-4.94
Fructose D	1	5.32
Gly	3	6.04
Zn^{2+} , SO_4^{2-}	1	-4.67
L-a-Ala	4	-6.05
L-Leu	1	4.04
L-Arg	5	4.41
L-Glu	2	-6.50
glucose	2	5.74
sucrose	3	-5.17
L-Pro	10	6.43

Conditions: CU: $5.00 \times 10^{-6} \text{ mol}\cdot\text{L}^{-1}$; CTS: $200 \text{ }\mu\text{g}\cdot\text{mL}^{-1}$; pH 2.50; BSA: $1.00 \times 10^{-8} \text{ g}\cdot\text{mL}^{-1}$

substances had little or no effect on the determination of proteins under the permission of $\pm 5\%$ relative errors, and thus the proposed method exhibits good selectivity in protein measurement.

Under the optimum conditions defined, the calibration graphs for BSA and HSA were obtained. They showed that there was a linear relationship between ΔI_f and the concentration of proteins listed in Table 2.

The proposed method was used for the determination of HSA in a real sample of people serum. The measured results match very well with those obtained from the UV spectrophotometric method, as shown in Table 3, while this method could achieve much lower detection limit.

The Interaction Mechanism

From the discussion above, it was concluded that BSA and CTS can both increase the fluorescence intensity (I_f) of CU. In the presence of CTS, the addition of BSA can greatly increase the I_f of CU. The maximum emission wavelength has blue-shift to 500 nm. This indicates the microenvironment changes of the system.

The Formation of CU-CTS-BSA System

The Resonance light scattering (RLS) technique is available to provide some insight into the process responsible for the formation of the complex, which is shown in Fig. 6. It can be seen that the RLS intensities of CU are enhanced when BSA and CTS are added into the CU system, especially since the RLS intensity of the CU-CTS-BSA system is the highest among all the studied systems. The RLS spectra are closely correlated to some intrinsic behaviors of the complex and reflect that a large CU-CTS-BSA ternary complex may be formed in the system.

According to the theory of RLS [20, 21], the peaks of light scattering at 292 nm and 375 nm in the systems are ascribed to the absorption bands of CU at 200–250 nm and 350–360 nm, respectively.

The Absorption Spectra of CU-CTS-BSA Complex

The absorption spectra of the systems are shown in Figs. 7 and 8.

According to the UV spectra of BSA (Fig. 7), the absorption peak at about 210 nm can reflect the framework conformation of the protein; the transition of aromatic heterocyclic residues such as tryptophan, tyrosine, phenyl-

Table 2 Analytical parameters

Excitation wavelength(nm)	Proteins	Linear range ($\mu\text{g}\cdot\text{mL}^{-1}$)	Correlation coefficient(r)	Limit of detection (S/N=3)($\text{ng}\cdot\text{mL}^{-1}$)
426	BSA	0.007–100	0.9927	3.96
	HSA	0.004–100	0.9966	2.46
280	BSA	0.007–100	0.9972	4.56
	HSA	0.01–100	0.9991	9.20

Conditions: CU: $5.00 \times 10^{-6} \text{ mol}\cdot\text{L}^{-1}$; CTS: $200 \mu\text{g}\cdot\text{mL}^{-1}$; pH 2.50

alanine (on the peptide bond of BSA) and so on are reflected by the absorption peak at 280 nm [22]. In this system, when CU and CTS are added into a protein solution, the peak of BSA at 210 nm decreases in intensity and the wavelength shifts to longer wavelengths; while the peak at 280 nm increases.

The above phenomena suggest that the interaction of CU, CTS and BSA may lead to substantial changes of protein conformation, and the major conformation may have reconstructed into a α -helix form, which is an unfolding process. Similar to cellulose, which is a linear polysaccharide [23], chitosan is strongly polar because of an amino group and a hydroxy group in its sugar residues. The amino group in chitosan molecule can bind with hydrophilic residue in protein molecules by forming strong intramolecular and intermolecular hydrogen bonds. At lower concentrations, chitosan molecular chains appear as stretch conformation and dilated linear molecular, which makes them interact with protein molecular sufficiently. Thus, chitosan chains can provide protein molecules with a hydrophobic environment, which may rapidly increase spiral components [24].

In addition, the red shift of the absorption peak indicates that the polarity of the microenvironment around BSA originating from CU-CTS decreased and so as the absorption at 280 nm increased.

From the absorption spectra of CU in the system in Fig. 8, it can be seen that CU has absorption at about 365 nm and 425 nm. With adding BSA and CTS, the absorption of CU at 430 nm has greatly enhanced while 365 nm decreased.

Table 3 The results of samples determination

Samples	Methods	Concentration ($\text{mg}\cdot\text{mL}^{-1}$)	Average($\text{mg}\cdot\text{mL}^{-1}$)	RSD(%)
HSA	This method	69.6, 70.0, 70.9, 69.7, 71.1	70.3	0.69
	UV method	68.6, 69.5, 67.7, 68.8, 69.4	68.8	0.72

Due to the electronic dipole allowed π - π^* type excitation in extended aromatic system, CU exhibits an intense, symmetrically-shaped absorption band in the visible region of 350–480 nm. Upon light absorption, a π electron is excited from the ground state to the first excited state and oscillates from one end of the chromophore to the other. If a bulky substituent is present on the central methylene carbon atom and sterically prevents the molecule from adopting a planar geometry, the maximum of light absorption shifts to the near-UV (354–366 nm) region and the molecule loses its color [25] since there is no conjugation between the two feruloyl parts. Based on these spectral analyses, it reasonably hypothesizes that in the CU-CTS-BSA system, a ternary complex CU-CTS-BSA formed. In formation of the complex, it is possible that chitosan and BSA combine with CU together through the carbonyl carbon in CU and thus make the planar structure of CU more rigid and stable.

Mechanism of Fluorescence Enhancement

Energy Transfer in CU-CTS-BSA

Figure 9 shows that with excitation at 280 nm, the emission peak of BSA is at 330 nm. When BSA is added into CU, its

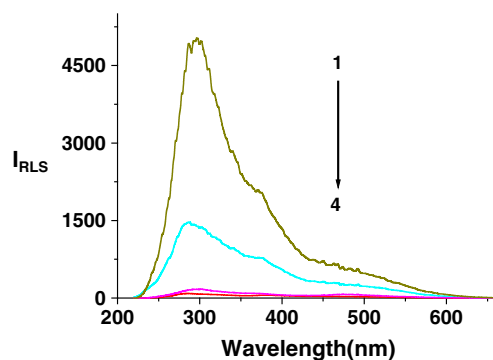


Fig. 6 Resonance light scattering spectra of: (1) CU-CTS-BSA, (2) CU-CTS, (3) CU-BSA, and (4) CU systems. Conditions: CU: $5.00 \times 10^{-6} \text{ mol}\cdot\text{L}^{-1}$; CTS: $200 \mu\text{g}\cdot\text{mL}^{-1}$; BSA: $100 \mu\text{g}\cdot\text{mL}^{-1}$ pH 2.50

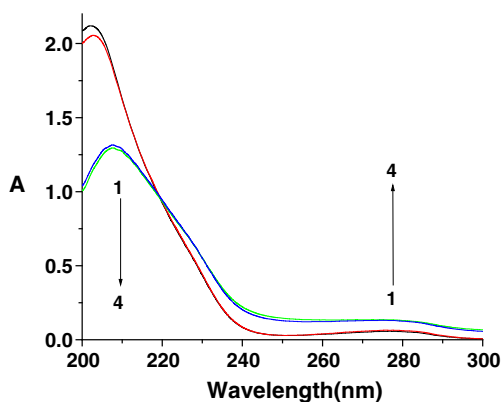


Fig. 7 The UV-visual absorption spectra of BSA of. (1) BSA, (2) CU-BSA, (3) CTS-BSA, and (4) CU-CTS-BSA systems. Conditions: CU: 5.00×10^{-6} mol·L⁻¹; CTS: 200 μg·mL⁻¹; pH 2.50; BSA: 100 μg·mL⁻¹

fluorescence decreases while the fluorescence emission of CU increases. Since there is an overlap between the absorption spectrum of CU and the emission spectrum of BSA (Fig. 10) thus an intermolecular energy transfer from BSA to CU exists under the excitation of 280 nm. When CTS is added into the system, the fluorescence of BSA is quenched and the characteristic fluorescence of CU is further highly enhanced, which reveals that energy of BSA is transferred to CU in the complex of CU-CTS-BSA. To understand this process, the energy transfer efficiency (E_a) and the interaction distance (r) between donor and acceptor can be evaluated using Förster theory [26, 27],

$$E_a = \frac{A_a}{A_d} \left(\frac{I_{ad}}{I_a} - 1 \right) \tag{1}$$

$$E_a = 1 - \frac{I_{da}}{I_d} \tag{2}$$

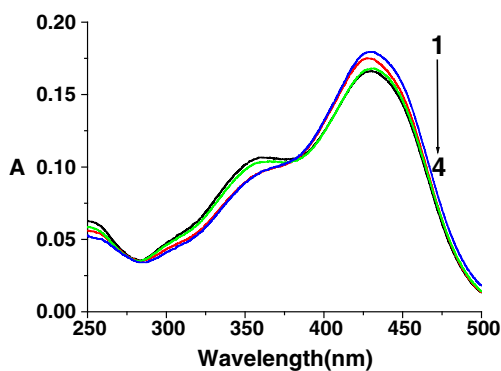


Fig. 8 The UV-visual absorption spectra of CU of. (1) CU-CTS-BSA, (2) CU-BSA, (3) CU-CTS, and (4) CU systems. Conditions: CU: 5.00×10^{-6} mol·L⁻¹; CTS:200 μg·mL⁻¹; pH 2.50; BSA: 100 μg·mL⁻¹

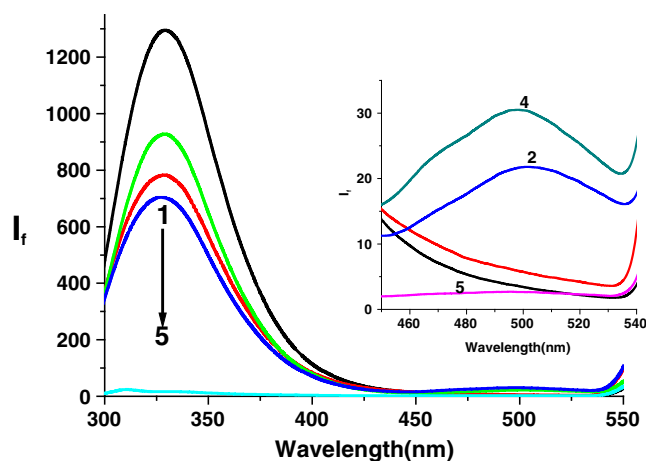


Fig. 9 The fluorescence spectra of BSA of. (1) BSA, (2) BSA -CU, (3) BSA -CTS, (4) CU-CTS-BSA, and (5) CU systems. Conditions: CU: 5.00×10^{-6} mol·L⁻¹; CTS: 200 μg·mL⁻¹; BSA: 100 μg·mL⁻¹; pH 2.50

$$R_0^6 = 8.8 \times 10^{-25} \cdot k^2 \cdot n^{-4} \cdot \phi_d \cdot J \tag{3}$$

$$E_a = \frac{R_0^6}{R_0^6 + r^6} \tag{4}$$

$$J = \sum F_D(\nu) \epsilon_A(\nu) \nu^{-4} \Delta \nu / (\sum F_D(\nu) \Delta \nu) \tag{5}$$

where the energy transfer efficiency E_a and the critical transfer radius R_0 are calculated, A_d and A_a are the absorbance of energy donor and acceptor, respectively; I_{ad} , I_a , I_{da} and I_d are the fluorescence intensities of the acceptor in the presence of donor, acceptor in absence of donor, donor in the presence of acceptor and donor in absence of acceptor, respectively. In Eq. 3 k^2 is a factor

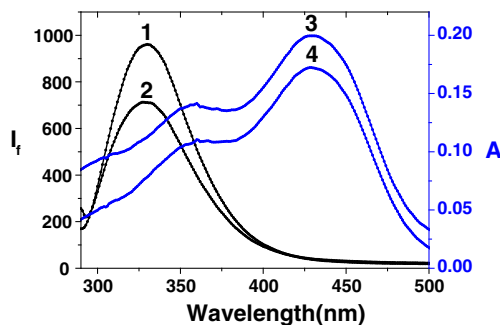


Fig. 10 Overlap between BSA (donor) emission and absorption of CU (acceptor). 1. BSA emission; 2. BSA-CTS emission; 3. CU-CTS absorption; 4. CU absorption. Conditions: CU: 5.00×10^{-6} mol·L⁻¹; CTS: 200 μg·mL⁻¹; BSA: 100 μg·mL⁻¹; pH 2.50

Table 4 Efficiency of energy transfer (E_a) and the critical transfer radius

System	Donor	Acceptor	E_a	$J(10^{-13}\text{cm}^6\text{M}^{-1})$	$R_0(\text{nm})$	$r(\text{nm})$
CU -BSA	BSA	CU	0.22	1.39	3.86	4.78
CU -CTS-BSA	BSA	CU	0.54	3.90	3.12	3.03

describing the relative orientation in space of the transition dipoles of donor and acceptor; ϕ_d is the fluorescence quantum yield of the donor in the absence of acceptor; n is the refractive index of the solvent; J is the spectral overlap integral between the emission spectrum of donor and the absorption spectrum of acceptor. The choice of Eq. 1 or Eq. 2 is based on the degree of the energy transfer efficiency in order to decrease calculated error. The values of E_a , R_0 and r are listed in Table 4.

In Table 4, it can be seen that in the binary complexes of CU-BSA, the energy transfer efficiency is low. In ternary complex of CU-CTS -BSA, the energy transfer is more efficient than that of the binary complex, which is the result of synergistic reaction among three substances. The distances between BSA and CU in ternary complex are decreased to 3.03 nm from 4.78 nm of binary complex. Therefore, with energy transfer efficiency increase, the fluorescence intensity of CU is greatly enhanced. So, it is concluded that the CTS molecule shorten the distance between BSA and CU, which promotes efficiency in energy transfer.

Define Fluorescence Quantum Yield and Fluorescence Polarization

As shown in Fig. 1, both BSA and CTS enhance the intrinsic fluorescence of CU at the emission peak of 530 nm. The intensity is greatly enhanced by BSA in the presence of CTS but the emission peak blue shifts to 500 nm. These changes may be related to the change in microenvironment for different systems. As shown in Table 5, the fluorescence polarization and quantum yield are different for the systems containing different components.

According to Perrin equation, the microviscosity of the microenvironment can be estimated using the fluorescence polarization of fluorescence probe [28]. A large value

Table 5 Fluorescence polarization (P) and quantum yield (Y) of the different systems

	CU	CU-CTS	CU-BSA	CU-CTS-BSA
P	0.140	0.266	0.393	0.397
Y	0.022	0.039	0.157	0.212

Conditions: CU: 5.00×10^{-6} mol·L⁻¹; CTS: 200 μg·mL⁻¹; pH 2.50; BSA: 100 μg·mL⁻¹

reflects a larger microviscosity than a low value. From Table 5, it is seen that the fluorescence polarization of CU in CU-CTS, CU-BSA and CU-CTS-BSA is increased gradually. This can explain why the absorption increases at 430 nm and decreases at 365 nm in the absorption spectra.

The fluorescence quantum yield of CU in the system is determined based on the reference method [29, 30] as shown in Table 5. The results show that the fluorescence quantum yield of CU increases to 0.212 in the CU-CTS-BSA system from 0.022 in aqueous. It is considered that the hydrophobic microenvironment of CTS-BSA can prevent the collision between CU and water, and decrease the energy loss of the CU-CTS-BSA system. The improved fluorescence quantum yield makes the fluorescence intensity highly enhanced for the CU-CTS -BSA system.

Conclusion

In this work, our studies showed that the fluorescence of CU can be highly enhanced by CTS and BSA, and the enhancement of fluorescence intensity is quantitatively proportional to concentration of proteins in a wide range. Based on this observation, a sensitive fluorescence method for determination of protein at nanogram levels is established, and evaluated by real samples, the HSA in human blood.

Mechanism studies show that in CU-CTS-BSA system, protein and CTS can bind together through hydrogen bond, and the BSA-CTS further combine with CU via center carbonyl carbon in CU. In this process, protein conformation changed from β-fold into α-helix, and a proper hydrophobic environment was provided to CU molecules. Thus, the fluorescence enhancement of CU is considered to originate from (a) the hydrophobic microenvironment provided by BSA and CTS, and (b) the intermolecular energy transfer between BSA and CU, in which CTS plays a crucial role because it shortens the distance between BSA and CU. Thus, the fluorescence quantum yield is improved and the fluorescence intensity of this system is significantly enhanced.

Acknowledgement The research is sponsored by Shandong Provincial Natural Science Foundation, China, through the project #Y2008B36.

References

1. Kragh-Hansen U (1981) *Pharmacol Rev* 33:17–53
2. Peters T Jr (1985) *Adv Protein Chem* 37:161–245
3. Carter DC, Ho JX (1994) *Adv Protein Chem* 45:153–203
4. Kumar CV, Buranaprapuk A (1999) *J Am Chem Soc* 121:4262–4270
5. Moreno F, Cortijo M, Gonzalez-Jimenez (1999) *J Photochem Photobiol* 69:8–15
6. Feng XZ, Lin Z, Yang LJ et al (1998) *Talanta* 47:1223–1229
7. Panjehshahin MR, Bowmer CJ, Yates MS (1989) *Biochem Pharmacol* 38:155–159
8. Macgregor RB, Weber G (1986) *Nature* 319:70–73
9. He XM, Carter DC (1992) *Nature* 358:209–215
10. Muzzarelli RAA (1977) *Chitin*. Pergamon Press, New York, pp 1–37
11. Roberts GAF (1992) *Chitin chemistry*. Mac Millian Press, Houndmills, pp 1–50
12. Kas HS (1997) *J Microencapsul* 14:689–711
13. Singla AK, Chawla M (2001) *J Pharm Pharmacol* 53:1047–1067
14. Kato Y, Onishi H, Machida Y (2003) *Curr Pharm Biotechnol* 4:303–309
15. Chandy T, Sharma CP (1990) *Biomaterials. Artif Cells Artif Organs* 18:1–24
16. Illum L, Jabbal-Gill I, Hinchcliffe M et al (2001) *Adv Drug Deliv Rev* 51:81–96
17. Krishnaswamy K, Raghuramulu N (1998) *Indian J Med Res* 108:167–181
18. Miquel J, Bernd A, Sempere JM et al (2002) A review. *Arch Gerontol Geriatr* 34:37–46
19. Zsila F, Bikadi Z, Simonyi M (2003) *Tetrahedron-Asymmetry* 14:2433–2444
20. Miller GA (1978) *J Phys Chem* 82:616–618
21. Pasternack RF, Bustamante C, Collings PJ et al (1993) *J Am Chem Soc* 115:5393–5399
22. Tao WS (1981) *Protein macular basic*. The People's Education Press, Beijing, p 256
23. Jiang TD (2003) *Chitin*. Chemical Industry Press, Beijing, pp 23–26
24. Zubay G (1989) *Biochemistry*. Fudan University Press, Shanghai, p 45
25. Pedersen U, Rasmussen PB, Lawesson SO (1985) *Liebigs Ann Chem* 8:1557–1569
26. Clegg RM (1995) *Curr Opin Biotechnol* 6:103–110
27. Kumara GA, Unnikrishnan NV (2001) *J Photochem Photobiol A* 144:107–117
28. Xu JG, Wang ZB (2006) *Fluorescence analytical methods*. Science Press, Beijing, pp 184–192
29. Wang F, Yang JH, Wu X et al (2006) *Anal Bioanal Chem* 385:139–145
30. Xu JG, Wang ZB (2006) *Fluorescence analytical methods*. Science Press, Beijing, pp 11–12